Development and operation of a material identification and discrimination imaging spectroradiometer

Mark Dombrowski

Surface Optics Corporation
9929 Hibert Street, Suite C, San Diego, CA, 92131

Paul Willson

U.S. Army Armament Research and Development Engineering Center
SMCAR-QAH-T, Picatinny Arsenal, New Jersey 07806-5000

Clayton LaBaw

Jet Propulsion Laboratory
4800 Oak Grove Drive, Pasadena, CA 91109-8099

ABSTRACT

Many imaging applications require quantitative determination of a scene's spectral radiance. This paper describes a new system capable of real-time spectroradiometric imagery. Operating at a full-spectrum update rate of 30Hz, this imager is capable of collecting a 30 point spectrum from each of three imaging heads: the first operates from 400 nx m to 950 nm, with a 2% bandwidth; the second operates from 1.5 μm to 5.5 μm with a 1.5% bandwidth; the third operates from 5 μm to 12 μm, also at a 1.5% bandwidth. Standard image format is 256 x 256, with 512 x 512 possible in the VIS/NIR head. Spectra of up to 256 points are available at proportionately lower frame rates. In order to make such a tremendous amount of data more manageable, internal processing electronics perform four important operations on the spectral imagery data in real-time. First, all data in the spatial/spectral cube of data is spectro-radiometrically calibrated as it is collected. Second, to allow the imager to simulate sensors with arbitrary spectral response, any set of three spectral response functions may be loaded into the imager including delta functions to allow single wavelength viewing; the instrument then evaluates the integral of the product of the scene spectral radiances and the response function. Third, more powerful exploitation of the gathered spectral radiances can be effected by application of various spectral-matched filtering algorithms to identify pixels whose relative spectral radiance distribution matches a sought-after spectral radiance distribution, allowing materials-based identification and discrimination. Fourth, the instrument allows determination of spectral reflectance, surface temperature, and spectral emissivity, also in real-time. The spectral imaging technique used in the instrument allows tailoring of the frame rate and/or the spectral bandwidth to suit the scene radiance levels, i.e., frame rate can be reduced, or bandwidth increased to improve SNR when viewing low radiance scenes.

The unique challenges of design and calibration are described. Pixel readout rates of 160 MHz, for full frame readout rates of 1000 Hz (512 x 512 image) present the first challenge; processing rates of nearly 500 million integer operations per second for sensor emulation, or over 2 billion per second for matched filtering, present the second. Spatial and spectral calibration of 65,536 pixels (262,144 for the 512 x 512 version) and up to 1,000 spectral positions mandate novel decoupling methods to keep the required calibration memory to a reasonable size. Large radiometric dynamic range also requires care to maintain precision operation with minimum memory size.

1.0 INTRODUCTION

Over the past three years, Surface Optics Corporation (SOC) has developed extensive experience in the field of real-time imaging spectroradiometry. During 1992, SOC developed a visible/near-IR band imaging

0-8194-1833-1/95/$6.00

spectroradiometer, capable of collecting a 30 point spectrum at each pixel in a 256 x 192 image in only 1/15th of a second. At the same rate that the instrument collects data, it also spectroradiometrically calibrates every point in the 1.5 million point cube of data; after data has been properly calibrated, each pixel's spectral radiance is then weighted by an arbitrary spectral response function and integrated spectrally, thereby allowing the instrument to emulate any VIS/NIR band sensor. Six such response curve convolutions can be performed simultaneously. Default curves produce the CIE tristimulus values on three channels, and RGB for display to a video monitor on the other three.

Building on the experience gained from this VIS/NIR imaging spectroradiometer, SOC has teamed with the Jet Propulsion Laboratory (JPL) to develop a second generation version of the VIS/NIR instrument. Capable of collecting up to 256 spectral points simultaneously from each of three spectral imaging heads covering the range from near-UV to long-wave IR, this new instrument implements real-time calibration and arbitrary response convolution, but also implements a much more powerful exploitation of the spectral data. A desired spectral radiance distribution may be entered into or measured by the instrument; by then selecting one of a wide variety of spectral-matched filtering algorithms, the instrument filters each pixel's spectral radiance against the sought-after radiance, showing matching pixels as bright, and mismatched pixel's as dim. Filtering algorithms range from very broad filters, requiring only basic similar shape for match, to very narrow filters, requiring close match of spectral features. The instrument is capable of collecting up to 30 spectral points from each head in only 1/30th of a second when using 256 x 256 imaging format, or up to 20 spectral points in the same time when using a 512 x 512 imaging format. Ultimate development of the instrument will also allow real-time compensation of atmospheric effects, and determination of temperature and spectral emissivity/reflectivity. SOC and JPL are currently working under contract with the U.S. Army Armament Research and Development Engineering Center (ARDEC) at Picatinny Arsenal to develop the first phase of this instrument, which will use one of the imaging heads to provide coverage from 1.5 μm to 5.5 μm.

2.0 INSTRUMENT DESCRIPTION

A detailed technical description of the instrument is presented below. Figure 1 presents a conceptual drawing of the ultimate 400 nm - 30 μm instrument, with three heads attached to a single processor. As illustrated schematically in Figure 2, basic design of a Multiband Identification and Discrimination Imaging Spectroradiometer (MIDIS) is straightforward, allowing construction of a compact, rugged, easily producible instrument. The instrument comprises four main sections. First, raw spectral images are gleaned by a continuously variable narrowband IR filter-based imaging spectrometer at up to a 1000Hz rate. Second, raw image data is collected, spectro-radiometrically calibrated, and processed by a high-speed processing section. Third, data is formatted as standard RS-170 analog video data or as high speed 12-bit digital data by an output processing section. Fourth, overall system operation is monitored and controlled by a system controller which also communicates to an external computer over standard serial or parallel busses.

All functions of the instrument, e.g, CVF speed, integration time, iris, have both an automatic and manual mode. In the automatic mode, the system controller determines the optimum settings for the instrument based on scene spectral radiances and dependent on other conditions already set by the operator, such as minimum allowable frame rate. In the manual mode, the operator sets the desired parameter to a given value through one of the interface busses, or through the back panel interface. These two modes allow for complete flexibility in instrument control, from fully autonomous operation, to completely manual control.

In either case, output from the instrument is fully spectro-radiometrically calibrated, unlike current spectro-radiometers which generally rely on an external computer for calibration and processing. Realizing that spectral images in-and-of themselves are only partially useful, SOC's instrument includes two very powerful processing modes. First, any desired spectral response function can be loaded into the instrument. Internal electronics will then integrate the product of the response curve and the measured spectral radiances to allow emulation of any type of SWIR/MWIR sensor system (or ultimately any VIS-LWIR sensor). Three such integrals can be performed and output simultaneously. Second is spectral matched filtering. In this mode, a desired relative spectral radiance to search for is either entered into, or measured by, the instrument.

Several internal matched filtering algorithms can then be employed to filter scene spectral radiances against the desired radiance; any objects in the scene possessing the desired relative spectral radiance will appear bright, while other objects will appear dim. Real-time preprocessing of the calibrated data will also allow determination of pixel temperature and spectral emissivity/reflectivity.

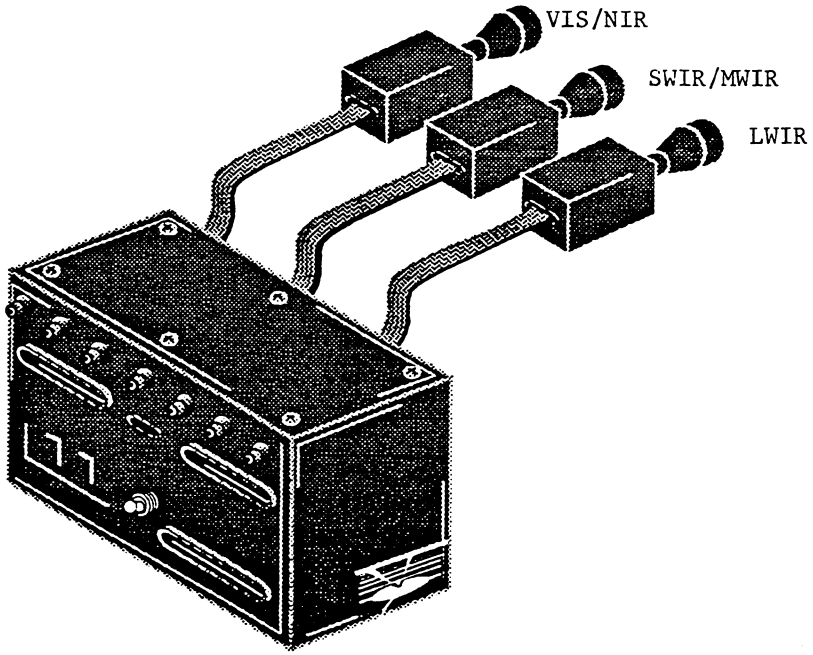

Figure 1. Multi-Band VIS-LWIR Imaging Spectroradiometer.

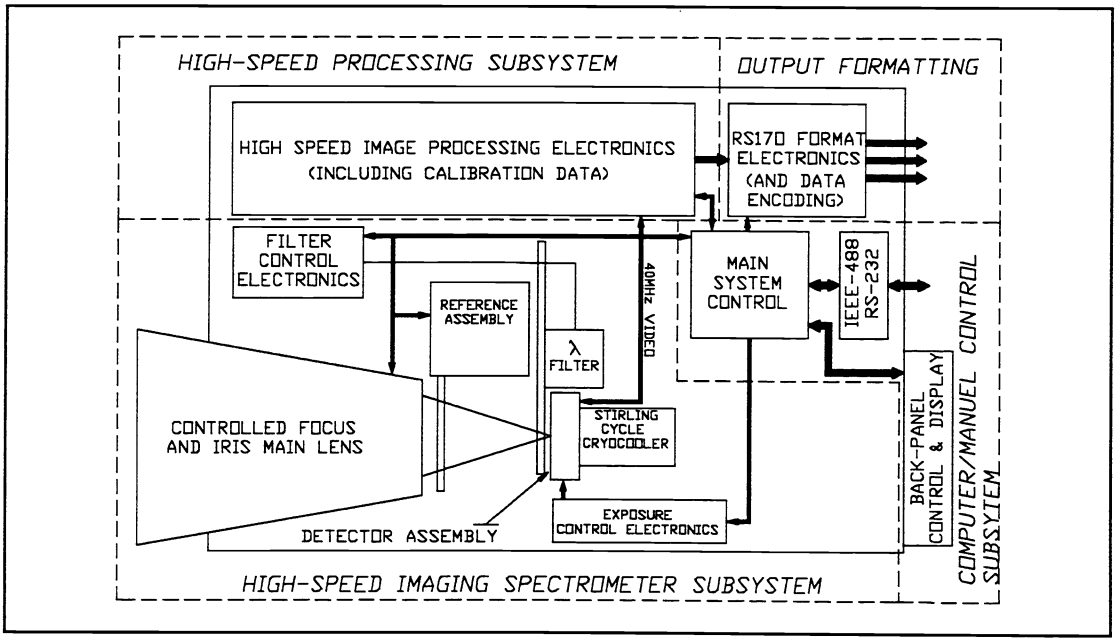

Figure 2. Schematic Overview of Imaging MWIR Spectroradiometer.

2.1 Imaging Spectrometer Detailed Description

The first step in generating and processing spectro-radiometric imagery is capturing raw spectral images. SOC and JPL are developing a circularly variable filter-based (CVF) spectral imager operating from about 1.5 μm to about 5.5 μm, analogous to SOC's already developed visible-band instrument.

2.1.1 Spectral Image Collection

Spectral information is gleaned by a narrow-band SWIR/MWIR circular variable filter. Comprising two segments, this filter varies its center wavelength from approximately 1.5 μm to 5.5 μm as it rotates 360°, and has a passband of approximately 1.5% FWHM of the center wavelength. Position of the filter is encoded to 4,095 points per revolution, ensuring accurate determination of exact wavelength being viewed. A 1.5% filter will see a negligible increase in its bandwidth when used in a fast F/1.8 system (cone angle =±15.5°). Hence, the imaging spectrometer portion of this instrument has tremendous light gathering capability. The CVF is also temperature stable, exhibiting a center wavelength change of only about 70ppm/°C, or only ±0.6% over the temperature range of -55°C to 125°C. This is less than half a bandwidth change, or only 15 nm at 2500 nm for extremely harsh environmental conditions.

Output from the CVF is imaged onto an area detector array, providing the spatial imaging of the system. The array is a 16-port 256 x 256, variable exposure, InSb array with a maximum exposure rate of 1,200 exposures per second. To compensate for band-to-band variances in spectral radiance and to effectively freeze the CVF's rotation, controllable integration time is necessary. Several different approaches can be used to effect variable integration time. In the visible band, this is simple task accomplished merely by gating on and off an image intensifier. In the infrared, such a technique can not be used since no photocathode material is available with a work function as low as a thermally-generated photon's energy. Mechanical shuttering could be used, but a shutter with the required aperture and response time (sub millisecond) would be extremely difficult to develop and likely unreliable; hence, this is not a viable option. Fortunately, electronic techniques can be used to effect variable integration time. The array is a random access photodiode array. Each photodiode integrates charge on an associated capacitor. Analog field-effect transistor switches then allow readout of each pixel. The array offers the ability to reset any sixteen pixels and read any other sixteen pixels in a 200ns clock cycle. Resetting pixels an appropriate number of clock cycles before reading them allows variable integration time. This can be visualized as a window moving through the array, with pixels at the leading edge of the window held in reset, pixels within the window integrating, and pixels at the trailing edge of the window being read out. Integration times are then variable from 1/4096th of the frame time up to the full frame time. At a frame time of 1.6 milliseconds, integration times are variable from 400 ns to 1.6 ms in 400 ns increments.

By placing the detector immediately behind the CVF, dramatic decrease in background noise is realized. Since the CVF achieves its blocking characteristics through reflection rather than absorption, emissivity of the filter is extremely low. Hence, background from the filter reaching the detector is minimal, since close proximity to the detector ensures that the detector sees its own reflection at only 77°K.

2.1.2 Internal Calibration Sources

To allow the instrument to maintain calibration with a minimal amount of laboratory calibration, MIDIS contains an internal reference. SOC is very familiar with the manufacture and use of blackbody sources, as much of our instrumentation employs these sources. For this instrument, a thermo-electrically controlled reference is employed. The reference consists of two blades connected to either side of the cooler; one cooler, then, produces both a hot and a cold reference, both of whose temperatures will be monitored to allow correct gain and offset compensation. Absolute spectro-radiometric calibration data is generated at time of assembly by having the radiometer view a source of known spectral radiance (blackbody). Immediately after this, the internal reference is viewed. By viewing the internal source later, calibration data can be appropriately scaled to compensate for any gain or offset variations.

2.1.3 Spectrometer Energy Throughput

In order to determine the expected performance of SOC's and JPL's proposed MIDIS, detailed analysis of the light gathering capability of the system was performed. Since such analysis is key to the expected performance of the instrument, a brief review of the throughput analysis will be conducted here. A short digression into radiometry will help to clarify how the instrument works. Assume that a detector of area A_p, linear dimension l_p, sits behind a lens of arbitrary focal length F and collecting area A_l, and is viewing a scene a distance D from the lens. Assume also that the scene possesses a spectral radiance $L(\lambda)$ in units of $W/(cm^2 \cdot sr \cdot \mu m)$. The lens will project the detector to an area A_{pp} on the scene. At a distance D from the scene, the lens subtends a solid angle Ω_l. Therefore, total power collected by the system and deposited, neglecting transmission or scattering losses, on the detector is $L(\lambda)A_{pp}\Omega_l$. Here, Ω_l was assumed small. If the angular distribution of radiance were to change significantly over the angle subtended by the lens, then explicit integration of spectral radiance over the lens's subtended angle would have to be performed. The preceding notation, however, is not easy to use since both A_{pp} and Ω_l depend on the distance D to the object. Introduce a new parameter, Ω_p, the solid angle subtended by the detector (pixel) at the focal distance from the lens. All these quantities are shown in Figure 3.

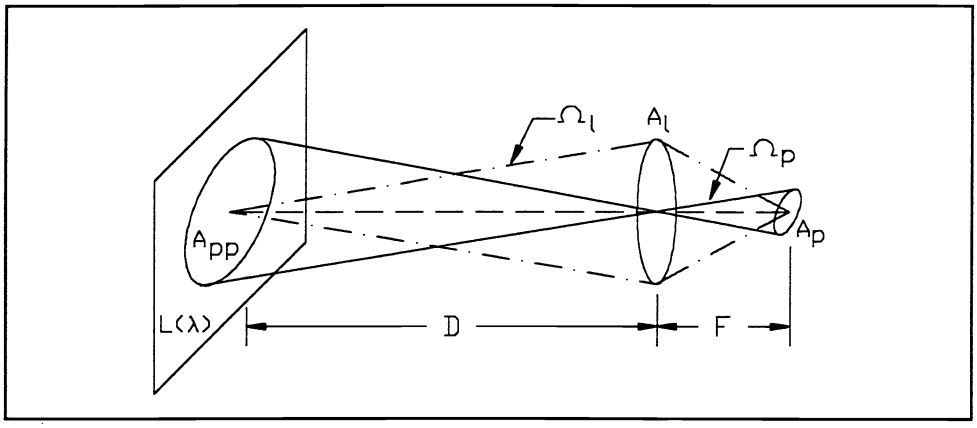

Figure 3. Definition of Terms for Energy Collection Analysis.

A simple derivation will show that given the condition of D >> F (i.e., image plane and focal plane of lens nearly coincident), and $l_p << F$, then the product $A_{pp}\Omega_l \approx A_l\Omega_p$, with the degree of approximation being dependent on the relative magnitudes of F, D, and l_p. For example, an F/1.8 lens with F = 55mm viewing a scene 1 meter away and illuminating a pixel 38 μm on a side, will have a $A_l\Omega_p$ product which is only .022% greater than the actual collection product of $A_{pp}\Omega_l$.

With the above description in mind, neglecting path radiance contributions for now, the spectral power incident on a given pixel in the imaging array, through an optical train of transmission $T_o(\lambda)$, through atmosphere of transmission $T_a(\lambda)$, but without any spectral filtering is

$$P(\lambda) = L(\lambda)\ \Omega_p\ A_l\ T_o(\lambda)\ T_a(\lambda) \qquad \left[\frac{W}{\mu m}\right] \quad .$$

If now a spectral filter with response function at λ_c of $F(\lambda,\lambda_c)$ is introduced into the optical train, the total power striking a pixel is

$$P(\lambda_c) = \int L(\lambda)\ A_l\ \Omega_p\ T_o(\lambda)\ T_a(\lambda)\ F(\lambda\ ,\ \lambda_c)d\lambda \qquad [W] \quad .$$

If the detector has a quantum efficiency $\eta(\lambda)$, and the pixel is exposed to the above power level for an integration time of Δt, then the total number of electrons collected by a pixel is

$$N_e(\lambda_c) = \int \frac{L(\lambda)\, A_l\, \Omega_p\, T_o(\lambda)\, T_a(\lambda)\, F(\lambda, \lambda_c)\, \eta(\lambda)\, \Delta t}{h\, \frac{c}{\lambda}} d\lambda \qquad [number] \quad .$$

Here, the division by hc/λ converts a spectral radiance to a spectral photon radiance. This is the desired throughput equation for a generalized spectro-radiometer. Also note that given a focal length F much greater than pixel dimension l_p, the product $A_l\, \Omega_p$ for a lens of f-number F/no can be rewritten as

$$A_l\, \Omega_p \approx \left[\frac{\pi\, l_p}{4\, F/no}\right]^2 \qquad [m^2 \cdot sr] \quad .$$

2.1.4 Spectral Imager Noise Levels

To correctly quantify system performance, an expression for the radiometer's noise level must also be generated. Four main sources were considered, namely signal shot noise, background shot noise, detector noise, and readout noise. Total noise, σ_{total}, is the RSS sum of these uncorrelated sources. By translating this RMS noise electron level back through the imaging system, a Noise Equivalent Spectral Radiance (NESR) can be generated as:

$$NESR(\lambda_c) = \frac{\sigma_{total}\, h \cdot c}{A_l\, \Omega_p\, \Delta t \int T_o(\lambda)\, T_a(\lambda)\, \lambda\, F(\lambda, \lambda_c)\, \eta(\lambda) d\lambda} \quad .$$

Figure 4 shows the target's spectral radiance and MIDIS's predicted NESR when viewing a 25°C sunlit grass field through a 1 km horizontal atmospheric path. Integration time is used as a parameter.

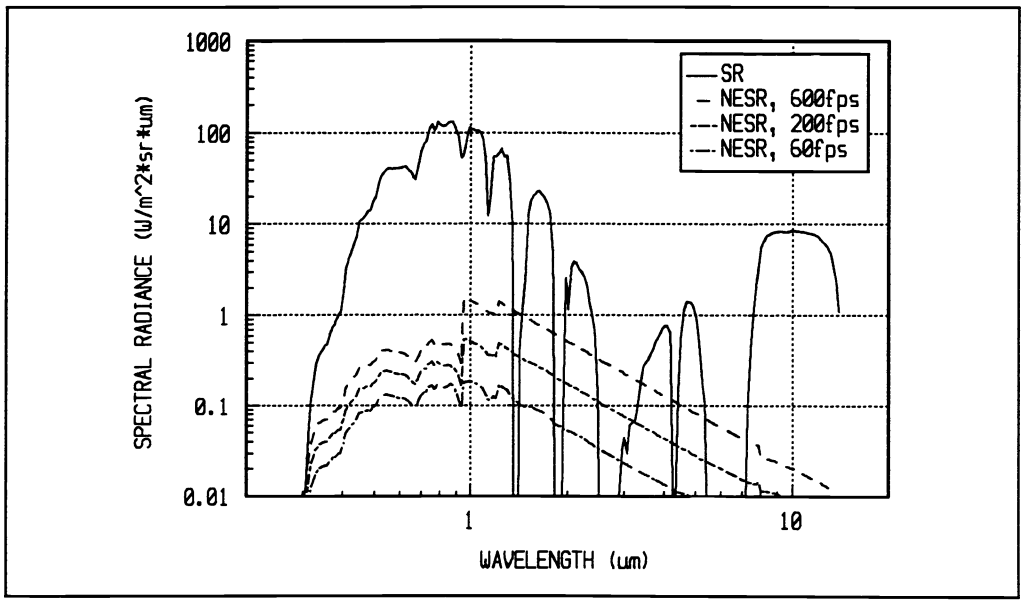

Figure 4. NESR and Target Radiance for Spectral Imager.

2.2 Processing Electronics

To this point, much explanation has been given to generating raw spectral images. Generation of images, however, is only a small part of the real goal of generating useful discriminants which can be used to classify, identify, track, or otherwise monitor a desired object. In order to generate useful discriminants from raw data, additional processing is necessary. Having a compact, high-speed spectral imager is of little use if a stand alone super-computer is necessary to process the data at the same rate as the imager generates it, or if a standard processor can process at only a fraction of the generation rate.

In order to effectively exploit the spectral images generated by MIDIS's imaging spectrometer, SOC's instrument includes a high-speed processing section. In addition to spectro-radiometrically calibrating each spectral and spatial pixel at the same rate that they are generated, the instrument further processes the spectrum for each spatial pixel, allowing real-time implementation of spectral response integration and spectral matched filtering. Pre-processing the calibrated data will ultimately allow real-time compensation for atmospheric effects and for determination of surface temperature and spectral emissivity/reflectivity. Spectral response integration allows the instrument to emulate any desired SWIR/MWIR imager by integrating the measured spectral radiances with any arbitrary response curve, so that the output at a given pixel, SE(p), is given by

$$SE(p) = \int L(\lambda, p)\, R(\lambda)\, d\lambda \quad ,$$

where $R(\lambda)$ is the spectral response curve of the sensor being emulated. SOC's visible-band instrument performs six such integrals simultaneously; MIDIS, however, performs three simultaneously. An even more powerful processing operation implemented by the instrument is spectral matched filtering. Here, a desired relative spectral radiance to filter for is loaded into the instrument, either by direct measurement or through an interface bus. Several different filtering algorithms with varying degrees of sensitivity can then be implemented to filter each pixel's spectral radiance against the sought after radiance, with matching pixels appearing bright, while mismatched pixels are dim. A few of the possible algorithms are described below.

The dot product is a very simple filtering algorithm that treats each spectral radiance as an N-dimensional vector and simply computes the dot product of the two vectors. Formally, this algorithm is given by

$$C_{DOT} = \frac{\sum L(\lambda_n) \cdot F(\lambda_n)}{\sqrt{\sum L(\lambda_n)^2 \cdot \sum F(\lambda_n)^2}} \quad ,$$

where $L(\lambda_n)$ is the measured spectral radiance at the n^{th} wavelength, and $F(\lambda_n)$ is the filter spectral radiance at the n^{th} wavelength. A major problem with this algorithm is that it is extremely broad. That is, the measured and filter radiances need only have roughly the same shape in order for the dot product to produce a high correlation value. The dot product generates the cosine between the two vectors acted upon by the algorithm. An N-dimensional vector can lie in any one of 2^N possible dimensional sectors, e.g., a three dimensional vector can lie in any one of 8 octants. Spectral radiances, however, are always positive, constraining radiance vectors to all lie in only one of their 2^N sectors. Hence, all vectors are necessarily forced to point in the same general direction, with the forced match becoming greater as more spectral points are added. How, then, can a tighter filter be implemented while still retaining spectral features?

The zero-mean dot product accomplishes this task. By removing the mean value from each spectral point, the shape of the spectral radiance curve is maintained, but the new zero-mean spectral radiance vector can now lie in any of the 2^N sectors of its N-space. Performing a dot product on the zero-mean radiance vectors then gives a tighter matching algorithm. This algorithm is given formally by

$$C_{ZMDOT} = \frac{\sum (L(\lambda_n) - \langle L(\lambda)\rangle)(F(\lambda_n) - \langle F(\lambda)\rangle)}{\sqrt{\sum (L(\lambda_n) - \langle L(\lambda)\rangle)^2 \cdot \sum (F(\lambda_n) - \langle F(\lambda)\rangle)^2}} \quad ,$$

where the spectral radiance mean is given by

$$\langle L(\lambda)\rangle = \frac{1}{N} \cdot \sum_{1}^{N} L(\lambda_n) \quad ,$$

and similarly for $\langle F(\lambda)\rangle$. Inspection of the above equation reveals that applying the zero-mean dot product to two spectral radiances is equivalent to treating those two radiances as sets of discrete random variables and computing the correlation coefficient between the two. Both the dot product and zero-mean dot product can also be applied to the derivative of the spectral radiances to further tighten their matching characteristics by simply replacing $L(\lambda_n)$ and $F(\lambda_n)$ in the above equations with $(L(\lambda_{n+1}) - L(\lambda_n))/(\lambda_{n+1} - \lambda_n)$.

In the infrared, the shape of the individual material spectral radiance curves is dominated by the shape of the Planck blackbody function, which reduces the efficacy of the spectral matched filter algorithms described above. To overcome this problem, MIDIS is being designed to ultimately allow real-time determination of surface temperature and spectral emissivity/reflectivity on a pixel-by-pixel basis. Using emissivity or reflectivity in place of true spectral radiance allows much more effective filtering based material characteristics.

These are but a few of the algorithms which SOC's MIDIS performs at the same rate at which image data is collected. Substantial computational power is needed to perform such processing. In fact, to spectro-radiometrically calibrated each pixel in a set of 256 x 256 pixel images 30 spectral points deep at each pixel, generated at 30Hz frame rate requires 131 million calculations per second. To calibrate the data and then evaluate three integrals of the form given by SE(p) above requires over 500 million calculations per second. To match filter using the most complex algorithm available to MIDIS and to perform response curve integration on three channels requires over 2.5 billion calculations per second. Compare this processing rate, albeit fixed-point, to a Cray 1S CFT capable of performing 23 million floating-point calculations per second and the magnitude of the challenge is evident. Electronics designed specifically to perform this task by using pipelined and paralleled processing yield the required processing speed.

3.0 MATCHED-FILTERING EFFICACY DEMONSTRATION

A major goal of the work performed during the phase I SBIR from ARDEC was to demonstrate the applicability and efficacy of spectral matched filtering to spatial contrast enhancement through exploitation of spectral features. Since all materials possess a relatively unique set of spectral complex indices of refraction giving rise to similarly unique spectral reflectances, emittances and transmittances, proper processing of spectral radiances allows material-based discrimination. If a material is to be uniquely identified, then explicit knowledge of the illuminant, of the material temperature, and of the transmittance of any intervening medium (such as the atmosphere) is required. In the case of laboratory or industrial measurements, these quantities can be controlled or directly measured. In the case of remote sensing, spectral distribution of illumination can be quantified fairly easily, and temperature and atmospheric transmittance calculated through appropriate processing. In the case of discrimination rather than identification, however, explicit knowledge of the material sought is not always necessary; rather, only a difference from another object is important. For instance, filtering for the measured radiance of, say, a grassy field will directly show all objects different from the field.

In order to demonstrate the increase in spatial contrast which can be obtained by matched filtering in the spectral domain, SOC procured material samples whose reflectances were measured to identify spectral

features that could be exploited using a spectral imaging camera. Computer simulations were performed to predict the performance of the imaging system and to develop and evaluate spectral processing algorithms. Two types of algorithms were evaluated: spectral matched filtering for spatially enhancing pixels with a desired reflectance spectrum in the image, and temperature and spectral emissivity determination from the pixel spectral radiance data in the image. Finally, a laboratory demonstration of infrared imaging spectroscopy was performed using a broad band, 3-12 micron, thermal imager and a series of discrete filters.

Through discussions with a firm that produces light weight, parabolic reflectors for space applications, graphite composite contamination was identified as an application that could benefit from use of spectral imaging. The manufacture of these reflectors requires surface preparation with chemical etching treatments. The residue left from the chemical etching process affects the adhesion and quality of the subsequent metal deposition on the reflector surface. An imaging spectroradiometer that could identify regions on the reflector surface that are contaminated with the chemical etch residue would be very valuable to quality control.

The composite manufacturer provided a number of samples of their graphite composite materials, some of which were known to be clean, and others known to be contaminated with a silica residue. Figure 5 shows a comparison of the 1.5 to 26 micron reflectance measurements of contaminated (FS6857) and clean (FS6855) samples of the graphite composite material, which shows significant variations in spectral emittance. A broad band, 8 to 12 micron, image of these samples is shown in Figure 6, and shows very little discernable contrast difference between the samples. Note that for display purpose, contrast of the printed image was increased four-fold. Using a spectral matched filtering algorithm, based on five experimental spectral points (4.4, 8, 9, 10.5, and 11.7 microns), demonstrated the capability for spatially enhancing features in the image with specific spectral properties. Figure 7 shows the filtered image using the five point filter derived from pixels on the contaminated sample (FS6857), which dramatically highlights the contaminated samples in the image; note that contrast of this image was not enhanced for printing, unlike the broad-band image. Also note that the two known contaminated samples show different distributions of contaminant; one shows blotchy contamination, while the other shows fairly uniform contamination. The sample on the far right was an unknown sample that also shows signs of contamination.

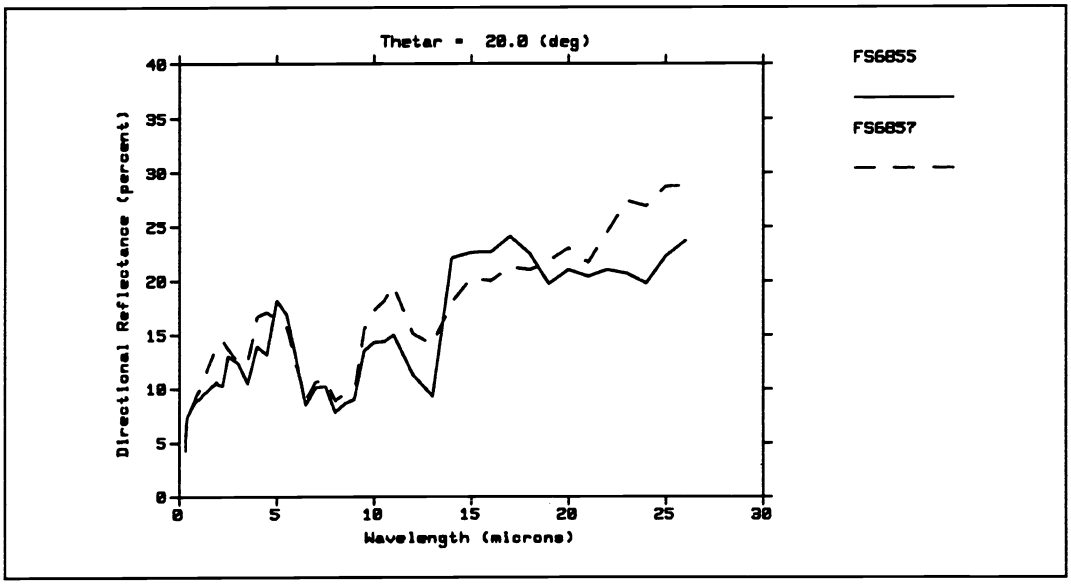

Figure 5. Comparison of a Clean (FS6855) and a Silica Contaminated Graphite Composite Sample (FS6854).

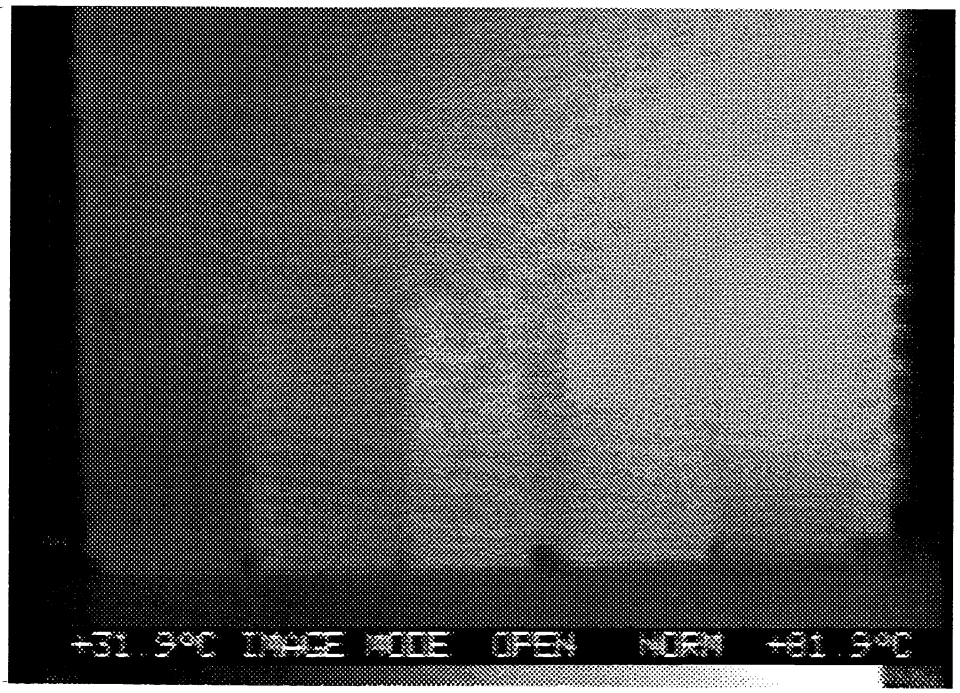

Figure 6. 8 μm to 12.0 μm Broad-Band Image of Graphite Composite Material.

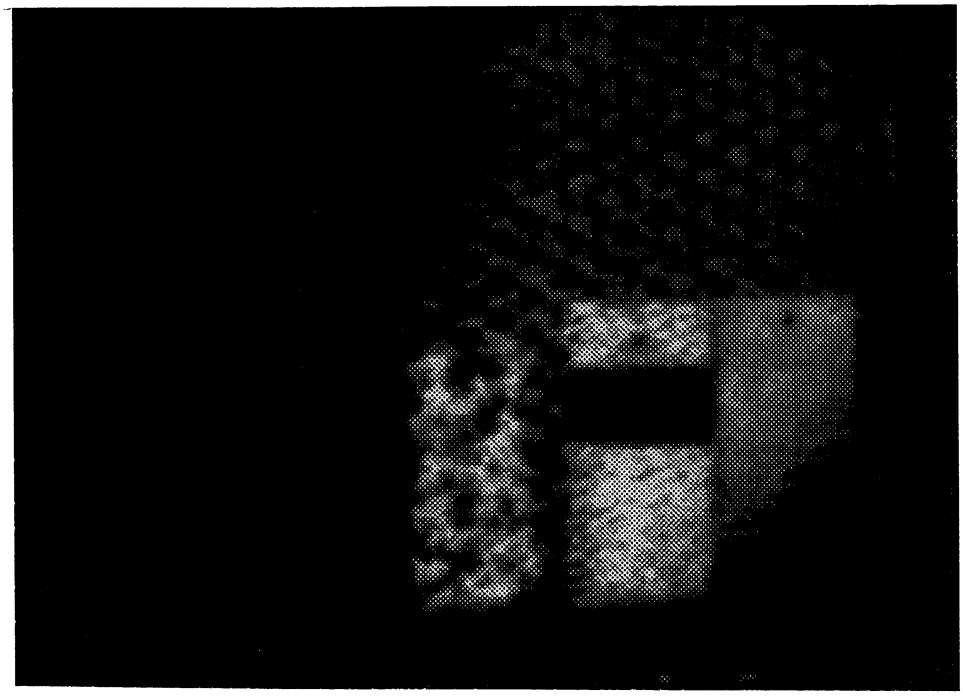

Figure 7. Filtered Image using FS6857 as Filter Spectral Radiance.

The laboratory demonstration of the use of infrared imaging spectroscopy for NDI applications that was performed during this Phase I program shows promising results. The spectrally filtered images, using one detector, five spectral points, and taking many hours to acquire and post process, clearly identified the regions in the image which matched the spectral filter. These results demonstrated only a small fraction of the capability of the proposed instrument with 256x256 detectors, 30 to 60 spectral points, and real-time processing and display.

4.0 CONCLUSIONS

Surface Optics Corporation and the Jet Propulsion Laboratory, under a phase I SBIR from the Armament Research and Development Engineering Center, have demonstrated the power of exploiting spectral features to enhance spatial contrast, allowing materials-based identification and discrimination. Embodied in a newly designed multiband, identification and discrimination imaging spectroradiometer (MIDIS), such capability will have broad benefit to any discipline requiring real-time remote identification of materials. For medical diagnostics, non-invasive identification of surface or near surface tissues will be possible without biopsy; with appropriate use of an endoscopic attachment, minimally invasive identification of internal tissues will also be possible. Remote monitoring of mineral deposits, crop type and health, or forest health will be possible more readily than with current instruments. Monitoring of industrial effluent discharge, or of toxic vapors from chemical spills will aid in protection of our environment and health. Similar monitoring could add another weapon to the arsenal in the war on manufacture of drugs. Any industry wanting to monitor processing of a product to increase quality and minimize cost would also benefit from the technology explored during this research and development, and currently being constructed.

5.0 ACKNOWLEDGEMENTS

Surface Optics Corporation is very grateful to the U.S. Army Armament Research and Development Engineering Center at Picatinny Arsenal for funding the Phase I SBIR under which the described research was performed. ARDEC's continued support in award of a Phase II SBIR to produce the MIDIS instrument researched during the Phase I effort will advance the state-of-the-art in real-time collection and processing of spectral imagery. SOC also thanks JPL for their support as subcontractor on this effort, lending their renowned experience and expertise in the field of spectral imaging.